



**QUEEN'S
UNIVERSITY
BELFAST**

Periodic transonic flow and control

Raghunathan, S., Early, J. M., Tulita, C., Benard, E., & Quest, J. (2008). Periodic transonic flow and control. *The Aeronautical Journal*, 112(1127), 1-16. <http://aerosociety.com/News/Publications/Aero-Journal/Online/314/Periodic-transonic-flow-and-control>

Published in:
The Aeronautical Journal

Document Version:
Peer reviewed version

Queen's University Belfast - Research Portal:
[Link to publication record in Queen's University Belfast Research Portal](#)

Publisher rights
EPSRC: * Author's final version (Required)

General rights
Copyright for the publications made accessible via the Queen's University Belfast Research Portal is retained by the author(s) and / or other copyright owners and it is a condition of accessing these publications that users recognise and abide by the legal requirements associated with these rights.

Take down policy
The Research Portal is Queen's institutional repository that provides access to Queen's research output. Every effort has been made to ensure that content in the Research Portal does not infringe any person's rights, or applicable UK laws. If you discover content in the Research Portal that you believe breaches copyright or violates any law, please contact openaccess@qub.ac.uk.

Periodic transonic flow and control

S. Raghunathan, J.M. Early, C. Tulita and E. Benard

School of Mechanical and Aerospace Engineering
Queens University
Belfast, UK

J. Quest

European Transonic Windtunnel
Cologne, Germany

ABSTRACT

The current understanding of periodic transonic flow is reviewed briefly. The effects of boundary-layer transition, non-adiabatic wall conditions and modifications to the aerofoil surface geometry at the shock interactions on periodic transonic flow are discussed. Through the methods presented, it is proposed that the frequency of periodic motion can be predicted with reasonable accuracy, but there are limitations on the prediction of buffet boundaries associated with periodic transonic flows. Several methods have been proposed by which the periodic motion may be virtually eliminated, most relevantly by altering the position of transition fix, contouring the aerofoils surface or adding a porous surface and a cavity in the region of shock interaction. In addition, it has been shown that heat transfer can have a significant effect on buffet.

NOMENCLATURE

c_θ chord length, m
 C_d drag coefficient $D/(\frac{1}{2}\rho U_\infty^2 c)$
 C_l lift coefficient $L/(\frac{1}{2}\rho U_\infty^2 c)$
 C_m moment coefficient $m/(\frac{1}{2}\rho U_\infty^2 c)$
 C_p pressure Coefficient $(p - p_\infty)/(\frac{1}{2}\rho U_\infty^2 c)$

D drag, N
 f frequency, Hz
 k non-dimensional frequency $\pi f c / U_\infty$
 L lift, N
 m moment coefficient
 M Mach number
 p local static pressure, N/m²
 p_∞ free stream static pressure N/m²
 Re Reynolds number $\rho_\infty U_\infty c / \mu$
 t time, s
 T adiabatic wall temperature, K
 T_r transition location as a percentage of chord
 T_w wall temperature, K
 U_∞ freestream velocity, ms⁻¹
 V local velocity, ms⁻¹
 v' fluctuating voltage, Volts
 x horizontal co-ordinate m
 X_s chordwise shock position on the surface
 y vertical co-ordinate, m
 ρ_∞ free stream density, kg/m³
 μ viscosity, kg/(ms)
 α Incidence angle, deg

1.0 INTRODUCTION

One of the major targets for aircraft designers within today's marketplace, as per the ACARE Vision 2020⁽¹⁾, is to increase aircraft safety five-fold by the year 2020. One of the key issues that need to be addressed in relation to safety is a full understanding of the mechanisms behind, and the methods of controlling, buffet at transonic speeds. Buffet excitation is typified by the pressure fluctuations originating from flow unsteadiness, and is associated with either boundary-layer separation or, in the case of transonic flows, self-excited periodic shock motion. Whereas the pressure fluctuations associated with boundary-layer separation are broadband in nature, the periodic motion, also commonly known as shock oscillations (or limit cycles), occurs at discrete frequency. The structural response to buffet excitation is known as buffeting and can lead to structural deformations and failure of both primary and secondary aircraft structures. In addition to the structural implications, buffeting also raises concerns with regard to aircraft performance and control.

The mechanism of the initiation and self-sustainability of shock oscillations has been a topic of research over several decades⁽²⁻⁴²⁾. The current understanding indicates that buffet excitation in transonic flows is initiated by shock-induced boundary-layer separation either on one surface of an aerofoil (for example, NACA0012), or on both surfaces when there is an asymmetry in shock positions (for example, a biconvex aerofoil at zero incidence) due to manufacture, slight incidence of airflow or the stagnation point not coinciding with the leading edge.

With regards to the mechanism of periodic motion on the lifting aerofoil, the shock induced separation on the suction surface leads to a rapid thickening of the boundary layer in the region between the foot of the shock and the trailing edge. In principle, this is equivalent to the sudden deployment of a flap at a negative incidence which reduces the effective camber sharply leading to the movement of the shock upstream.

Figure 1⁽²⁷⁾ depicts the initiation of periodic shock oscillations over a NACA 0012 aerofoil during rapid pitching, in which the aerofoil moves from a regime of steady transonic flow into the periodic flow regime through the change in airflow incidence. The methodology used here was to (1) perform a time accurate computational analysis of the flow over the aerofoil at an incidence, just below that where shock oscillations were known to occur, (2) to rapidly pitch the aerofoil about the quarter chord, into a regime where shock oscillations were known to occur, pitched in real time but with a total pitching time period much smaller than cyclic period, and (3) to compute the flow field again. Figure 1a shows the shock position as a function of iterations, NITS (time). Although pressure distributions were computed every ten time steps, only

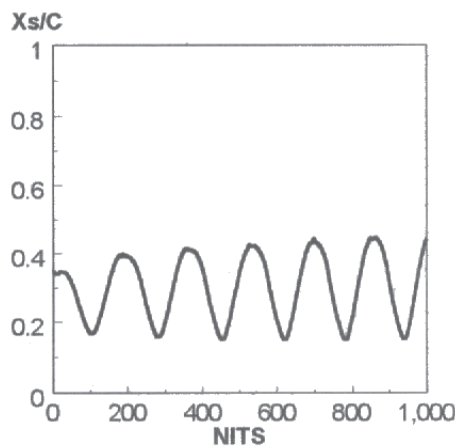


Figure 1(a). Shock position on NACA0012 aerofoil pitched up from 5° to 6° in 1/16th of the periodic time ($M = 0.7$, $R = 10 \times 10^6$, $Tr = 3\%$)⁽²⁷⁾.

alternate frames every 20 time steps are shown in Fig. 1(b) (cf. Fig. 1(a)). The formation of a shock-induced bubble can be seen in frame 3 (NITS 20), while frames 3 to 11 show the movement of the shock upstream and the enhanced separation behind the shock during this part of the cycle, as inferred from the trailing edge pressures. This is followed by a reattachment of the boundary layer (frame 13) that should lead to an effective positive camber. This configuration at this freestream condition is unstable for the shock wave, which then moves downstream (frames 15 to 19). The cycle then repeats itself.

There are two opposing effects of the shock moving upstream (frames 3 to 11). The upstream movement of the shock, on a quasi steady basis, should lead to a reduction in the shock Mach number and shock induced separation. On a dynamic basis, the movement of the shock upstream should increase the velocity relative to the shock and the shock Mach number, leading to an increase in shock induced separation (frame 11). The net effect during the upstream motion of shock appears to be that the shock strength slightly reduces and the flow remains separated. The Mach number contours during a cycle of periodic motion on a supercritical aerofoil⁽⁴²⁾ also support the above hypothesis. It should be noted that in addition to the above, there is a phase difference between the shock motion and state of the boundary layer in the region between the shock, the trailing edge and the wake. Furthermore, at low Reynolds numbers relative to the freestream flight conditions, the process is further complicated by the fact that there could be a trailing edge separation.

In order to develop an understanding of the mechanism of shock oscillations on biconvex aerofoils, a procedure was developed⁽²⁹⁾ in which (1) the flow was computed around the aerofoil with a splitter plate extension, which converged to steady state solution, (2) the splitter plate was removed instantly and (3) the flow was computed as the shock oscillations developed. Figures 2 depict the behaviour of the flow from the time the splitter plate is removed. After an initial period, depicted in Fig. 2(a), the shock becomes periodic. Mach number contours shown in Fig. 2(b) correspond to the specific time steps shown in Fig. 2(a).

As shown in Frame 1 (Fig. 2(b)), there are no shock oscillations present at the start of the cycle. At 170 time steps (frame 2), the shock has moved forward on the upper surface and rearward on the lower surface. It is suggested that there is an asymmetric separation at this stage. Between 170-250 time steps (frames 3-4), the shock on the upper and lower surfaces move in opposite directions, with the shock on the upper surface moving downstream with reduced separation, and that on the lower surface moving upstream with continued separation.

At time step 250, the direction of shock motion changes. On the lower surface, the shock is at the most rearward position at time step 360.

The energy transfer for the process is understood to be as follows⁽²⁸⁾: the periodic motion of the shock leads to the development of a periodic wake. The downstream movement of the shock produces pressure waves (Fig. 3) that interact with the trailing edge and propagate upstream. The interaction of these waves with the shock leads to an energy transfer that sustains the shock motion.

The characteristic features of transonic periodic flows⁽²⁻⁴³⁾ may be inferred from investigations to date, and are summarised as follows:

- (i) The buffet excitation due to transonic periodic flows on aerofoils is confined to a single frequency and occurs over a narrow range of Mach numbers;
- (ii) The frequency of periodic motion is directly related to the time required for the signals to travel from the mean shock position to the trailing edge;
- (iii) The onset of buffet corresponds to shock induced separation;
- (iv) On bi-convex aerofoils, shock waves move in anti-phase on the upper and lower surfaces during shock oscillations;
- (v) The periodic flows can be modified, or even disappear, if the shock interaction occurs in the vicinity of boundary-layer transition, and;

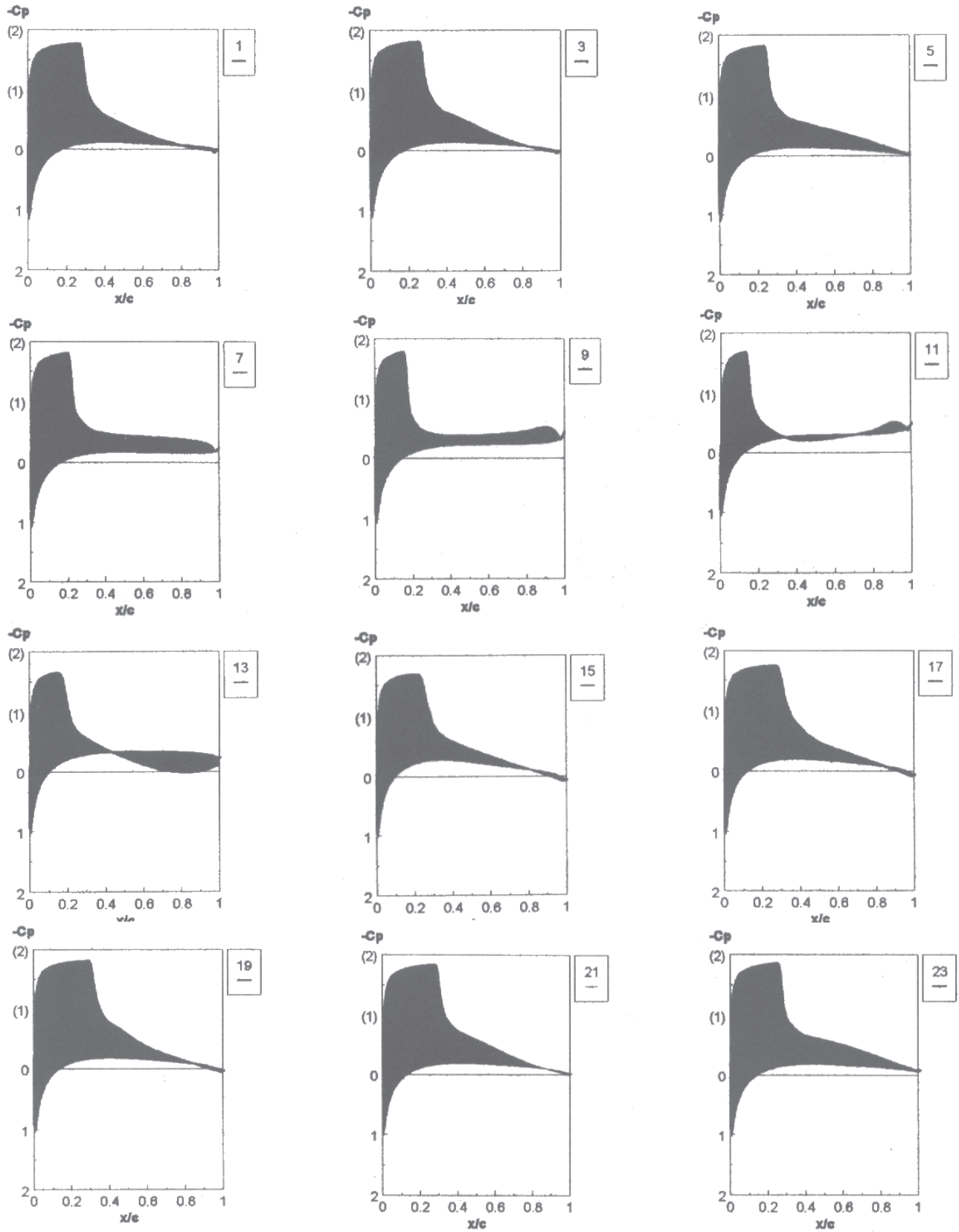


Figure 1(b). Pressure distributions at every 20 time steps on the NACA0012 aerofoil pitched from 5° to 6° incidence, $M = 0.7$, $Re = 10 \times 10^6$ (refer to Fig. 1(a))⁽²⁷⁾.

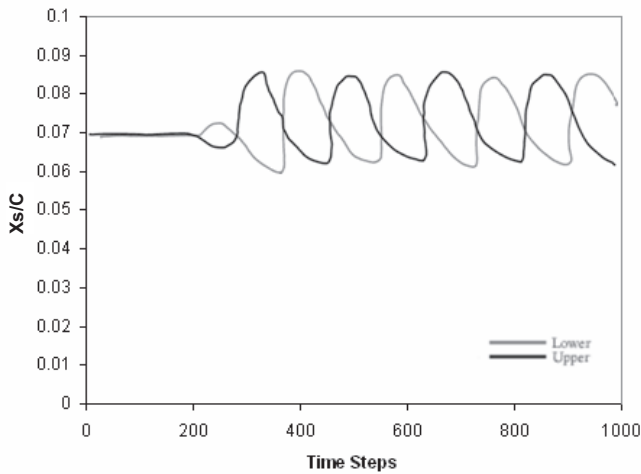


Figure 2(a). Transonic Periodic Flow on a 18% thick biconvex aerofoil, $M = 0.771$, $Re = 10 \times 10^6$, $\alpha = 0^\circ$, shock positions on upper and lower surface⁽²⁹⁾.

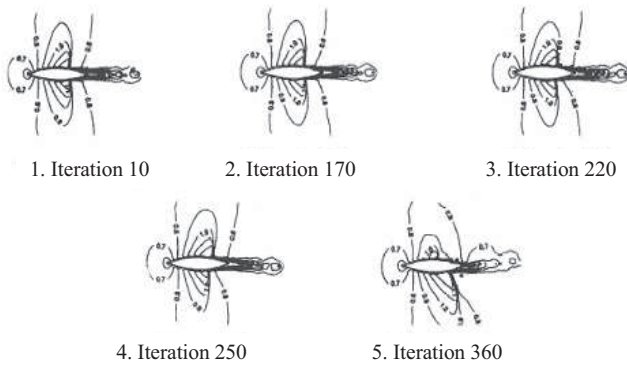


Figure 2(b). Transonic Periodic Flow on a 18% thick biconvex aerofoil, $M = 0.771$, $Re = 10 \times 10^6$, $\alpha = 0^\circ$, fixed transition⁽²⁹⁾.

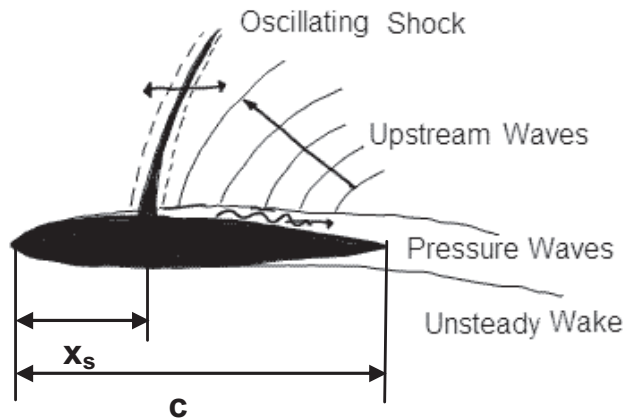


Figure 3. Mechanism for energy transfer due to wave propagation during periodic transonic flow⁽³¹⁾.

(vi) There are three types of shock motion on an aerofoil, which are known as Tidjeman Type A, B and C⁽⁴⁾

Tidjeman Type A shock motion is a small amplitude, almost sinusoidal, motion. Type B shock motion is of relatively larger amplitude and is characterised by the disappearance of the shock wave during a part of the cycle. In the case of Type C shock motion, the amplitude of the shock motion is even larger again, and propagates upstream into the freestream as a weak and shock-free wave during a part of the cycle.

Additionally:

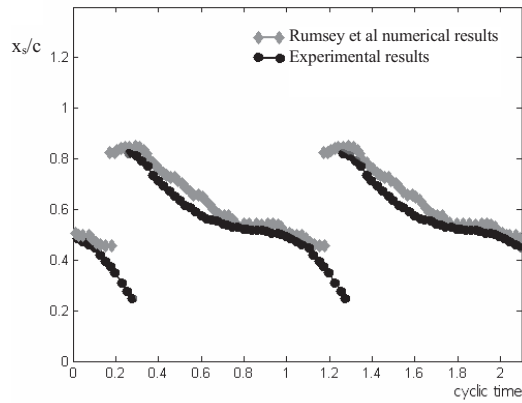
- (vii) The Mach number range for the periodic motion, with a fully turbulent boundary layer on the aerofoil surface, is virtually independent of the Reynolds number;
- (viii) On NACA0012 and supercritical aerofoils, shock oscillations occur at non-zero incidence and with shock motion on one side of the aerofoil only. The reduced frequency of oscillations is typically half of those for the bi-convex aerofoil;
- (ix) For a three-dimensional wing of varying chord, the frequency of buffet excitation may be composed of several frequencies, and can be attributed to varying chord along the span;
- (x) In free flight, the inherent shock oscillations may be partially attributed to interaction with aircraft motion and angle-of-attack changes.

In the paper, the methods available for predicting the periodic motion over an aerofoil are reviewed briefly, the effects of boundary transition and non-adiabatic wall conditions on periodic motion are discussed, and the results of investigations into the use of a bump, or a dimple, as means for alleviating the buffet associated with periodic transonic flows are presented.

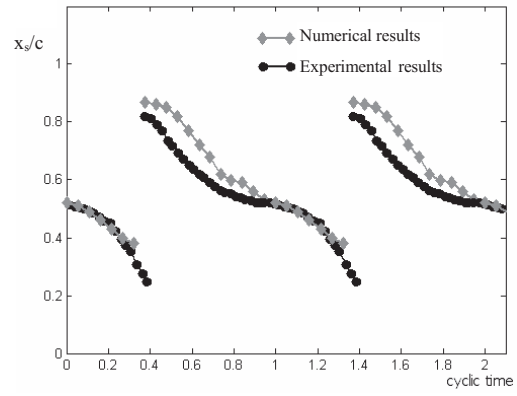
2.0 PREDICTION OF PERIODIC TRANSONIC FLOW

The aerodynamic performance of an aerofoil/wing subject to transonic periodic flows can be described by the onset of buffet, its amplitude, frequency and boundaries. The challenges in predicting buffet due to periodic motion^(2,9,22,24,31-35) include (a) identification of a well-defined buffet boundary, (b) capturing the correct Tidjeman's type of shock induced oscillation, (c) capturing the correct location of the oscillatory region on the surface of the aerofoil, and (d) accurate prediction of the reduced frequency. The accuracy of the predictions by CFD depends on both the turbulence model and the temporal/spatial accuracy of the shock-capturing numerical discretisation scheme used, while the experimental results are subjected to wind-tunnel constraints. The early investigations reported in the 1970s on transonic periodic flow^(2,3) were on a bi-convex aerofoil, with the numerical methods based on MacCormack's explicit scheme with an algebraic eddy viscosity turbulence model. It was concluded from this work that the use of a better turbulence model based on steady flow experiments can improve the predictions.

The current CFD techniques for prediction of periodic transonic flows^(2-9,22,24,31-35) are primarily based on two methods. The first method consists of solving the time accurate Reynolds Averaged Navier-Stokes (RANS) equations^(24,26,29,38,40) directly using an implicit or explicit numeric scheme in conjunction with algebraic or non-linear turbulence models (or, more recently, using Large Eddy Simulation, LES). The second method is the interactive boundary-layer coupling method^(15,22) and involves the solution of an outer inviscid region and an inner viscous boundary-layer which is coupled through the boundary condition on the wing and wake. The effect of the turbulent viscous boundary-layer is modeled at each time step in the quasi-steady manner by solving a set of ordinary differential equations for the integral boundary-layer quantities. In order to enhance the time accuracy in shock capturing, both strategies employ sub-iterative techniques in the context of a multi-grid methodology.



(a)



(b)

Figure 4. Shock location on the upper-surface of an 18% thick bi-convex aerofoil during periodic motion. (a) $M = 0.76$, $Re = 10 \times 10^6$, $k = 0.49^{(24)}$, (b) $M = 0.76$, $Re = 10 \cdot 10^6$, $Tr = 3\%$ chord, $k = 0.48^{(40)}$.

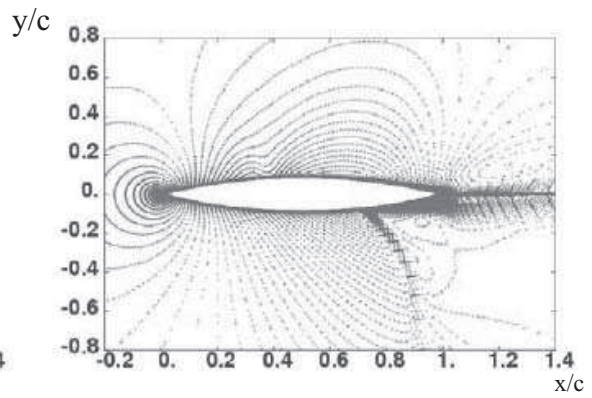
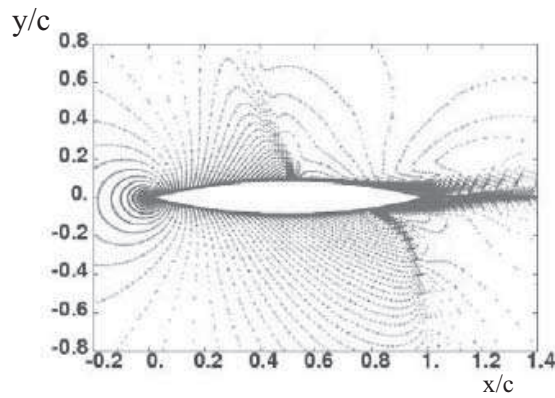


Figure 5. Mach number contours at two instants of time on 18% thick bi-convex aerofoil showing Type C motion ($M = 0.76$, $Re = 10 \times 10^6$, $\alpha = 0^\circ$, $Tr = 3\%$ chord, $k = 0.48^{(40)}$).

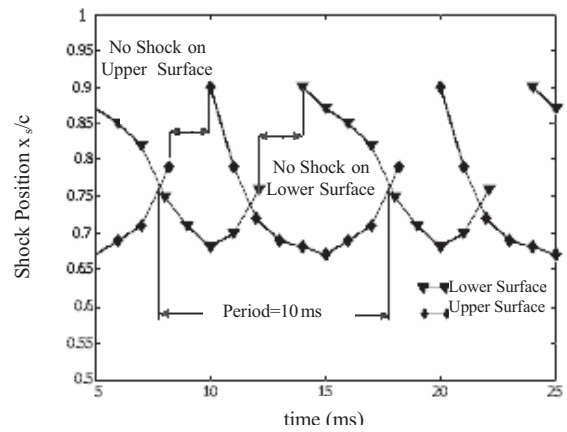
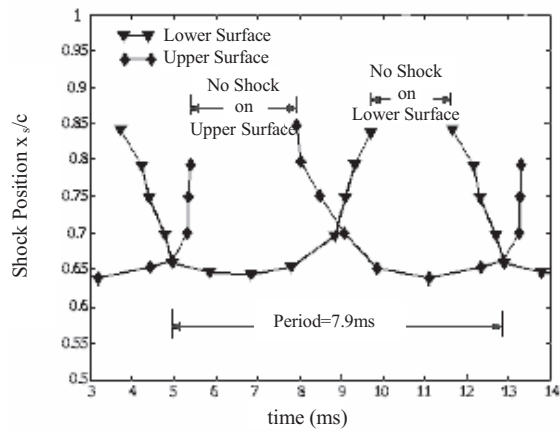


Figure 6. Shock location on the upper-surface of a 14% thick bi-convex (a) experimental results ($M = 0.85$, $Re = 7 \times 10^6$, $\alpha = 0^\circ$, $k = 0.5$, Ref. 19), (b) Predictions ($M = 0.83$, $Re = 9 \times 10^6$, $\alpha = 0^\circ$, $k = 0.47$).

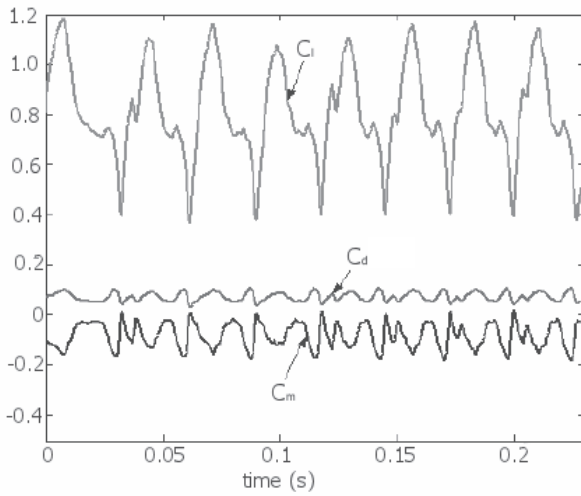


Figure 7. Predicted aerodynamic force coefficients during transonic periodic flow over a supercritical aerofoil⁽⁴⁰⁾.

2.1 RANS approach

The RANS approach, which relies on approximate algebraic and one/two equation turbulence models, has been widely used successfully in numerical prediction of periodic transonic shock motion on circular, NACA0012 and supercritical aerofoils. Typical examples of this approach in predicting shock position and reduced frequency can be seen in the work on a bi-convex aerofoil^(24,26,40), a NACA0012 aerofoil^(29,38,42) and a supercritical aerofoil^(35, 38).

2.1.1 Bi-convex aerofoil

Computation of periodic flow over an 18% thick bi-convex aerofoil is shown in Fig. 4. Prediction (Fig. 4(a)) reported by Rumsey *et al*⁽²⁴⁾ used both the Baldwin-Lomax and the Spalart-Allmaras⁽⁴⁷⁾ models. Predictions (Fig. 4(b)) was based on an implicit and explicit method, in conjunction with Roe's flux-difference-splitting shock-capturing scheme and where all viscous terms were centrally-differenced⁽⁴⁰⁾. The prediction methods, in the case of implicit schemes, took into consideration the importance of sub-iterations in enhancing the time accuracy of conventional implicit schemes^(44,45), and in the case of explicit schemes, practical time steps with a five-stage Runge-Kutta time marching scheme. The turbulence model used in the above cases was the Baldwin-Lomax⁽⁴⁶⁾ scheme. It can be observed that for both cases there are some differences between experiments and predictions for the range of chordwise shock motion over the aerofoil.

At $M = 0.76$ ⁽²⁴⁾, with the Spalart-Allmaras turbulence model, the predicted values of reduced frequency were in the range of 0.46 to 0.5, compared to the experimental value of 0.49. Further, the hysteresis effects observed experimentally in earlier works were reproduced numerically by using the correct grid size and time step in conjunction with several sub-iteration types. However, the value predicted by Rumsey *et al*⁽²⁴⁾ for reduced frequency with the Baldwin-Lomax turbulence model was much lower than the predicted value of 0.48 reported in Ref. 40 with the same turbulence model. The importance of turbulence modeling, coupling between the turbulence modelling and the shock capturing, the mesh and the turbulent transition in predicting separated flows has been highlighted by several researchers^(6,50,51).

The differences in the predicted value for the non-dimensional frequency between the investigations reported in Refs 24 and 40, even though both employed the same turbulence model, can be explained through the different dissipative mechanism used in the finite difference and finite volume schemes (FDS and FVS). The work reported in Fig. 24 used Roe's shock capturing scheme, whereas the work in Fig. 40 was based on the same turbulence

model in conjunction with an upwind van Leer implicit predictor/corrector cell-centered finite volume, second order time accurate scheme^(45,48) with two sub-iterative steps⁽⁴⁹⁾. The numerical dissipation in the finite difference schemes is basically inconsistent with the Navier-Stokes viscous terms, leading to the numerical shock instability and the so-called odd-even decoupling which could generate spurious solutions, whereas the form of the numerical dissipation in the FVS is consistent with the Navier-Stokes viscous terms. The predictions of Mach number contours which show the shock waves (Figs 5), infer that the periodic motion is of the Type C.

A further example is the prediction of shock position for periodic flow on a 14% thick aerofoil⁽³⁹⁾ compared with the experiments of Fig. 12 is shown in Fig. 6. Experiments (Fig. 6(a)) were conducted at $M = 0.85$, $Re = 7 \times 10^6$ and zero degrees incidence with transition fixed at $x/c = 0.02$. The computed results (Fig. 6(b)) were at different conditions: $M = 0.83$, $Re = 9 \times 10^6$ and zero degrees incidence with transition fixed at 3% chord. In terms of transonic flows, the difference in Mach number of 0.02 is significant, and therefore the comparison can be viewed as qualitative. In both cases, it can be observed that Tijdeman's Type B periodic motion was detected during a part of the oscillation cycle on upper or lower aerofoil surface in the upstream phase, the shock wave intensity decreases considerably and the shock wave almost disappears. The calculated reduced frequency based on semi-chord was 0.47, compared to an experimental value of 0.5.

2.1.2 NACA 0012 aerofoil

In the case of the NACA0012 aerofoil with a RANS approach, all three kinds of periodic motion were identified on the upper surface of the aerofoil ranging between Mach 0.7 and 0.8, at different angles of incidence and Reynolds numbers based on chord ranging from 1 to 14×10^6 ⁽³⁸⁾. For example, at $M = 0.775$, $Re = 10 \times 10^6$ and four degrees incidence with a Baldwin-Lomax turbulence model, a type B periodic motion was observed. The reduced frequency was $k = 0.23$, compared with 0.22 found by Edwards with an interactive boundary-layer approach⁽²²⁾. The shock motion was in the range of 15% to 40% chord.

Predictions of buffet boundaries for periodic flow on NACA0012 aerofoil by Barakos and Drikakis⁽⁴¹⁾, based on nonlinear two-equation low Reynolds number eddy viscosity turbulence models in conjunction with a functional coefficient for eddy viscosity, agreed well with experiments of McDevitt and Okuno⁽¹³⁾.

2.1.3 Supercritical aerofoil

Predictions, based on RANS approach with Baldwin Lomax turbulence model for periodic flow over the LV2F aerofoil⁽⁵⁰⁾ at $M = 0.74$, $R = 10 \times 10^6$ and incidence at 4 degrees are shown in Figs 7 and 8. Transition was fixed at 32% chord on both surfaces. The variation with time of the aerodynamic coefficients (Fig. 7) indicates a high level of buffet. The variation in the lift coefficient is $\pm 50\%$, and correspondingly, there is a large variation in both moment and drag coefficients.

The Mach number field around the LV2F aerofoil at four time instants during a cycle (Fig. 8) shows a significant variation in the shock position which is consistent with the large variations in the lift coefficient. The disappearance of shock (Type B) during a part of the cycle is also seen in this figure. The reduced frequency based on chord is 0.54 compared with the value of 0.48 obtained experimentally⁽⁵⁰⁾. There were differences in prediction of the range of shock motion – while the numerical location of the oscillatory region on the aerofoil has been found between 28% and 58% chord, the experimental indicates the location is between 32% and 55% chord.

The flow unsteadiness on the LV2F aerofoil discussed above can be observed in Fig. 9. Experimental velocity voltage fluctuations traces (Fig. 9(a)) for the aerofoil were obtained with free transition⁽⁵⁰⁾ and at several chord wise positions by surface mounted cryo

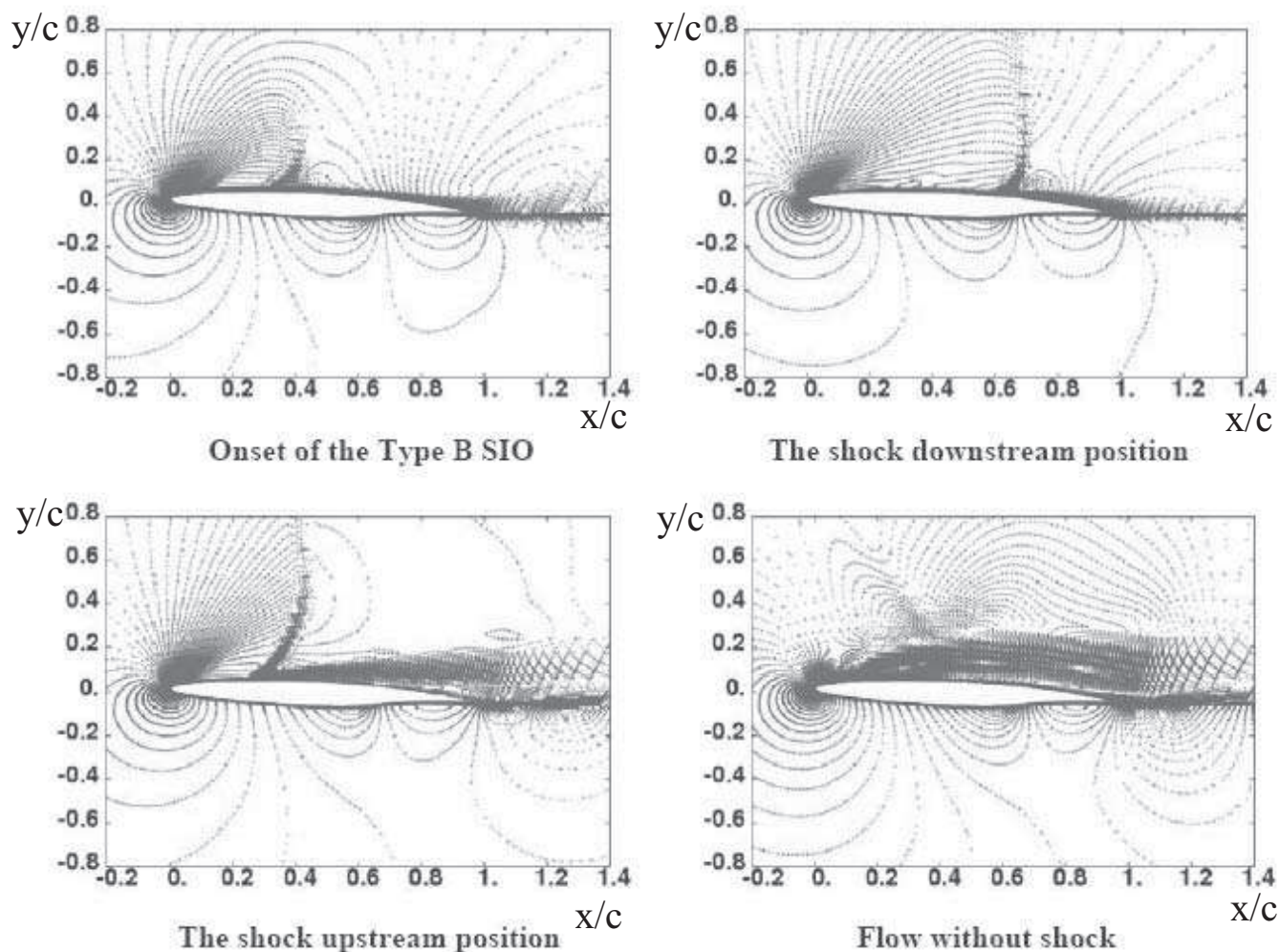


Figure 8. Predicted Type B periodic motion on LV2F aerofoil. ($M = 0.74$, $Re = 10 \times 10^6$, $\alpha = 4^\circ$, $k = 0.54$). Tr at 32%⁽⁴⁰⁾.

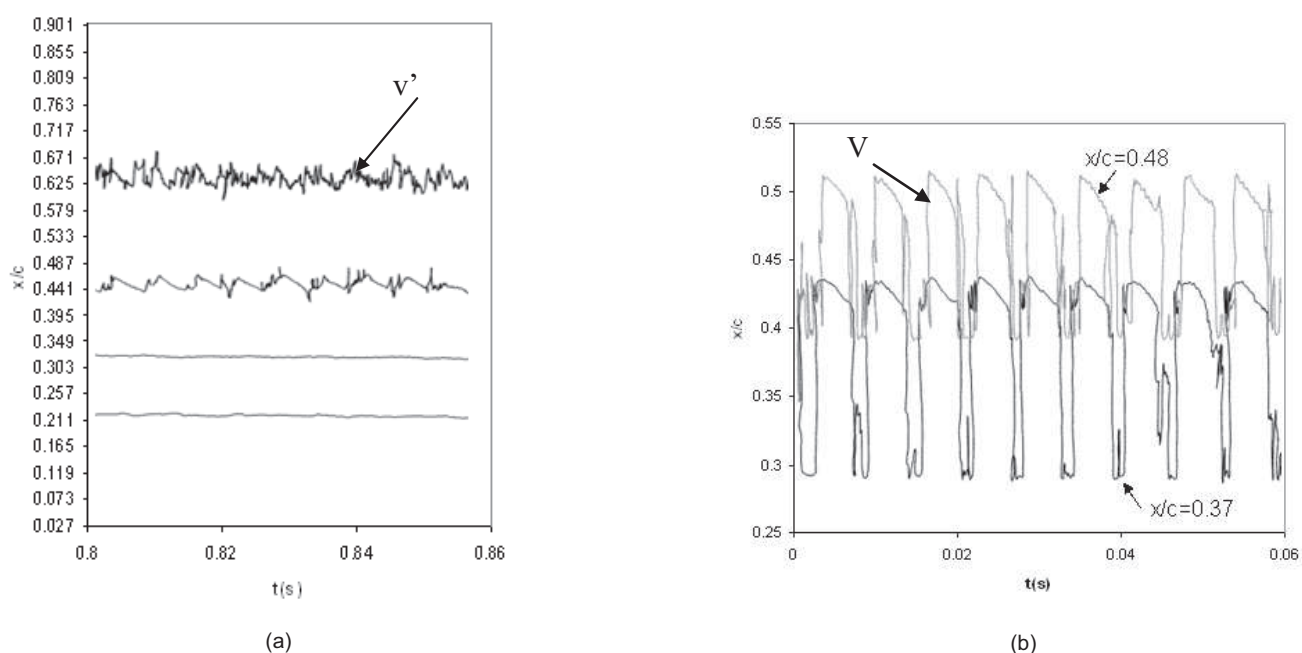


Figure 9. The flow unsteadiness on the LV2F aerofoil. (a) Schematic of experimental anemometer traces⁽⁵⁰⁾ and (b) numerical calculations on LV2F aerofoil⁽³⁴⁾ ($M = 0.74$, $Re = 10 \times 10^6$, $\alpha = 4^\circ$, $k = 0.54$).

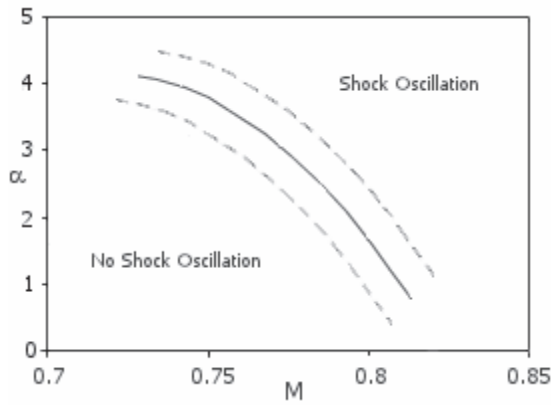
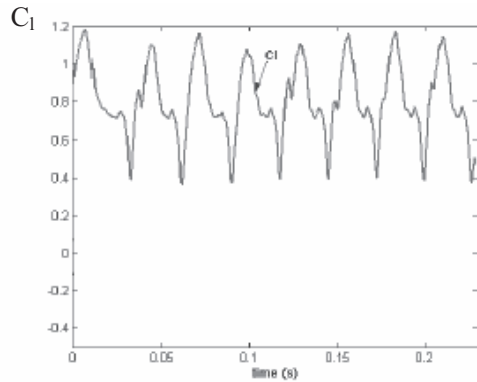
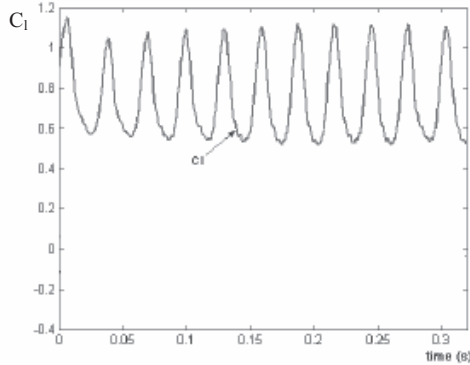


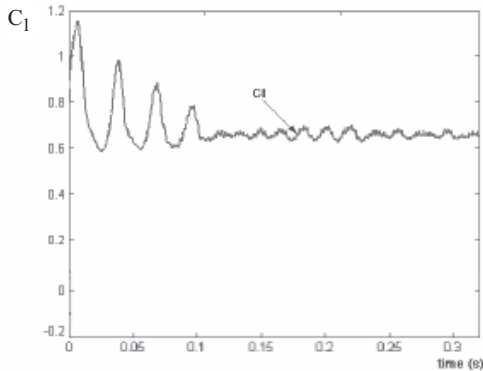
Figure 10. Buffet boundaries for NACA0012 (based on Refs 12, 26, and 40).



(a) $Tr = 32\%$



(b) $Tr = 7\%$



(c) $Tr = 18\%$

Figure 11. Effect of transition fix on periodic motion ($M = 0.74$, $Re = 10 \times 10^6$, $\alpha = 4^\circ$, based on Ref. 40).

hot-films. These devices are often used in conventional wind-tunnels and free-flight tests to measure wall stress and determine transition location on the model or the flight test vehicle. The numerical velocity results⁽⁴⁰⁾, shown in Fig. 9(b), calculated from surface pressures at two chordwise locations agrees qualitatively with the experimental data. The continuous change in the unsteadiness levels observed can be associated with periodic motion of the shock.

Predictions on a BGK no 1 supercritical aerofoil⁽⁴²⁾ using a RANS approach with a $k-\omega$ turbulence model also showed a good agreement with the experiments in describing the mechanism for energy transfer for the periodic shock motion. The predictions confirmed that the pressure waves propagate downstream from the shock wave within the separated region and on reaching the trailing edge they are reflected as an upstream-moving wave outside the separated region. The non-dimensional periodic frequency based on the sum of the time taken for the waves to move towards the trailing edge and back was 0.175 compared with that based on the Fourier analysis of the lift coefficient of 0.16.

2.2 Boundary-layer interactive approach

An alternative to solving the RANS equations directly is the interactive boundary-layer method^(10,15,22). In Edwards' method⁽²²⁾, the coupling between the inner viscous boundary-layer solution and the solution of the outer inviscid region is accomplished through the boundary conditions on the airfoil and wake. The potential code CAP-TSD employed by Edwards⁽²²⁾ contained modifications developed by Batina⁽⁵²⁾ to approximate the effects of shock-generated entropy and vorticity. From the leading edge of the airfoil, the boundary layer was approximated by the turbulent boundary layer with a prescribed pressure distribution. This assumption is suitable for an attached flow boundary layer, where the effect of the turbulent viscous boundary layer is modeled in the quasi-steady manner by the integral boundary-layer lag entrainment method of Green *et al.*⁽⁵¹⁾. When flow separation occurs, a boundary-layer velocity profile proposed by Melnik and Brook⁽⁵²⁾ is employed in an inverse boundary-layer approach.

The coupling between the inverse boundary layer and the inviscid solution is accomplished using Carter's method⁽⁵⁵⁾, calculating the displacement thickness in conjunction with a set of coupled ordinary differential equations (ODEs) in time at each chord-wise location. Calculation of the boundary-layer equations in the wake uses an exponentially decaying wake velocity profile shape in modelling the upper and lower wake surfaces.

Edwards employed this algorithm to compute the buffet onset boundary and the main characteristics of periodic motion at different turbulent regimes for the 18% thick bi-convex aerofoil and NACA0012 aerofoil⁽²¹⁾.

A comparison of interactive boundary layer with the RANS approach with variants in $k-\omega$ turbulence model on both conventional and supercritical aerofoil by Bartel⁽³⁵⁾ and the work of Edwards⁽²²⁾ indicates that the interactive boundary-layer coupling methods lead to results that are comparable with those obtained by the most expensive Navier-Stokes codes using the RANS/LES/DNS turbulence methodologies. Further, it should be emphasised that predictions generated by the RANS method are sensitive to the turbulence model employed (see, for example, Ref. 41).

The results of various prediction methods, including the RANS and Edwards coupling methods shown in Fig. 10, appear to be in fair agreement with the experiments for the buffet boundary of the NACA0012 aerofoil in the range $M = 0.75$ to 0.85 . The dotted lines in Fig. 10 indicate the range uncertainty in predicting the buffet boundaries ($\alpha = 1^\circ/M = 0.05$). It should be emphasised that the experimental results are subject to tunnel wall interference and flow disturbances in the tunnel. Indeed, comparison of experiments on transonic periodic flow on bi-convex aerofoil performed in a wind tunnel with both hard walls and walls with an acoustic

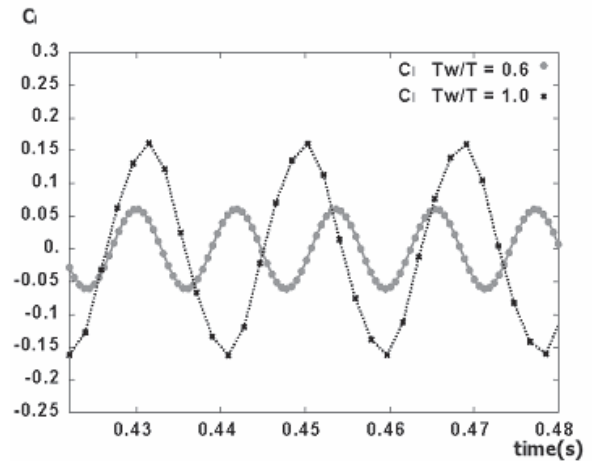
treatment have shown significant differences in buffet levels and buffet frequency⁽¹²⁾. Within the limitations of CFD, in particular the specification of the exact boundary conditions, predictions with tunnel constraints (particularly with slotted walls) can be performed only to the first order of accuracy. A potential way forward for the improvement of such predictions would be to perform such experiments in a contoured wall wind-tunnel and validate the experimental results with CFD, taking in consideration the boundary-layer development on all of the walls.

3.0 THE INFLUENCE OF THE BOUNDARY-LAYER TRANSITION ON PERIODIC MOTION

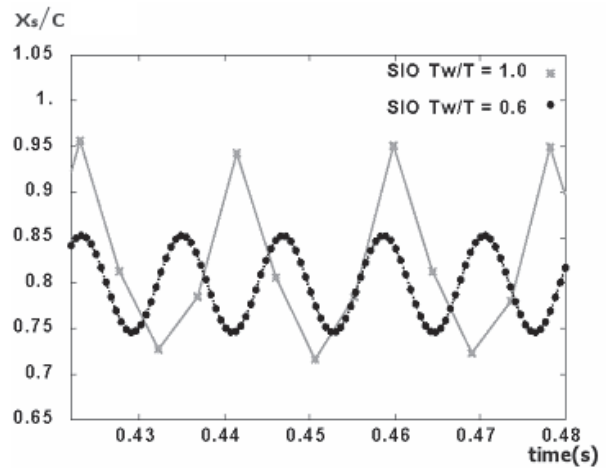
All the predictions of periodic transonic periodic flows on aerofoils discussed above are based on the assumption that the flow over the aerofoil is essentially turbulent i.e. the transition is fixed near the leading edge. Wind-tunnel testing on models in low Reynolds number wind-tunnels, in order to simulate higher Reynolds numbers, are often conducted with fixed transition near the leading edge of the model. However, the high Reynolds number European Transonic wind tunnel (ETW) does allow simulation of free flight with free transition. One of the reasons for the differences observed between predictions and experiments for the amplitude, range and frequency of shock motion could be due the differences in transition locations.

The effect of transition location on aerofoil lift coefficient for periodic transonic flows, based on RANS approach with Baldwin Lomax turbulence model on LV2F supercritical aerofoil, can be seen in Fig. 11. The results shown here are for $M = 0.74$, $Re = 10 \times 10^6$, $\alpha = 4$ deg, $T = 288K$ and for three transition locations of 32% (Fig. 11(a)), 7% (Fig. 11(b)) and 18% chord (Fig. 11(c)) respectively. Some of these results are compared qualitatively with the transition free experiments conducted in the pilot transonic wind tunnel (PETW) at the European transonic wind tunnel (ETW) facility (Fig. 9(a)) where the transition was observed to be between 15 to 20% chord.⁽⁵⁰⁾

The occurrence of periodic motion on the LV2F supercritical aerofoil with a transition fix at 32% can be seen in both Figs 7 and 11(a), where the periodic motion as can be inferred from the fluctuations in lift coefficient and is of large amplitude (Type B). For this case, the numerical chordwise location of the oscillatory region on the aerofoil has been found to lie between 28% and 58%. With transition fixed at 7% chord (Fig. 11(b)), the periodic motion is of a relatively of smaller amplitude. However with transition fixed at 18% (Fig. 11(c)), it is observed that the numerical values of periodic lift converges with time steps to a level which is relatively small. Earlier experiment on bi-convex aerofoils and at low Reynolds numbers^(8,18) showed that if the transition were to occur in the region of shock oscillations, the periodic motion would disappear. Although that is not exactly observed here with respect to the chordwise location of transition, the order of magnitude of changes produced due to the change in transition location is observed to be large. This indicates that the periodic motion is very sensitive to the transition location, particularly if the transition were to occur not too far upstream of the upstream position of the shock wave during the periodic motion. A plausible explanation for this is that a rapid change in the boundary-layer displacement thickness due to transition is equivalent to a sharp change in the effective geometry, almost like placing a wedge or a bump on the surface. This should generate an oblique shock wave at the location of the change in geometry and thus making it stable. Further investigations are needed in order to confirm this.



(a)



(b)

Figure 12. Effect of cooling on lift and shock motion 14% bi-convex aerofoil ($M = 0.83$, $Re = 9 \times 10^6$, $\alpha = 0^\circ$, $Tr = 3\%$ chord, Refs 22, 40).
(a) Variation of Lift, (b) Shock Position.

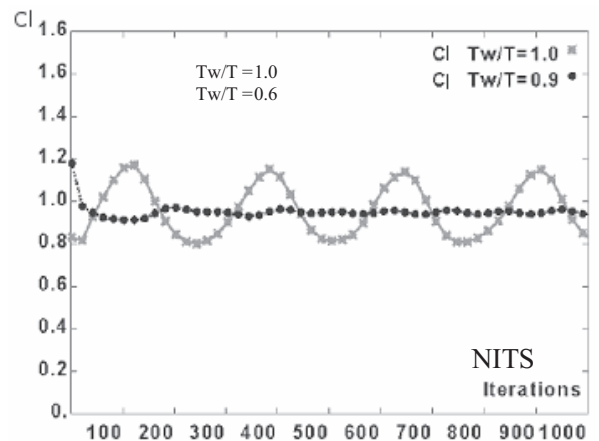


Figure 13. LV2F – Effect of cooling on lift on LV2F aerofoil ($M = 0.74$, $Re = 20 \times 10^6$, $\alpha = 4^\circ$, Refs 22, 40).

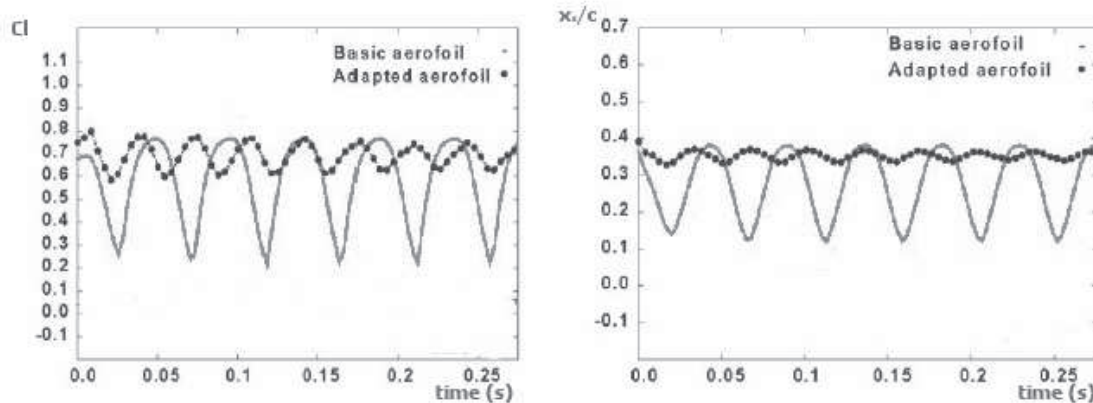


Figure 14. Alleviation of periodic over a NAA0012 aerofoil with a bump present: $M_\infty = 0.7$, $Re = 9 \times 10^6$, $\alpha = 3.2^\circ$ depicting: a Lift, b shock motion.

5.0 THE EFFECT OF HEAT TRANSFER ON PERIODIC MOTION

A substantial body of work exists on the effect of heat transfer on steady subsonic boundary layers⁽⁵⁷⁻⁶⁰⁾. The heat transfer between the aerofoil and the flow field has an important influence on the laminar and/or turbulent boundary-layer development, boundary-layer transition, boundary-layer separation and shock boundary-layer interaction⁽⁶³⁻⁶⁶⁾. It is understood that the surface heat transfer has a significant effect on the shockwave-boundary-layer interaction and on the skin friction at the surface of the aerofoil. In supersonic regions, the dominating effect of heat transfer is through viscosity (cooling decreases the viscosity and therefore the skin friction), whereas at subsonic speeds the dominating influence of heat transfer is through the velocity gradients (cooling increases the velocity gradients and, correspondingly, the skin friction). Cooling also has a significant effect on periodic transonic flows^(21, 29, 39).

Heat transfer effects are related to the temperature of the wall relative to the adiabatic temperature. With a wall temperature lower than the free stream total temperature, energy is transferred to the layer near the wall which results in a transfer of energy towards the wall. This transfer ultimately results in an increase in the velocities and velocity gradients normal to the surface at close proximity to the wall. Furthermore, the layer near the wall has also has a higher density relative to the freestream flow. Due to the combined effect of the higher density and velocity near the surface, a large increase in mass and momentum of the flow is promoted. The displacement thickness is primarily controlled by the mass flow near the wall and therefore decreases with cooling. The fuller velocity profile leads to a decrease in the shape factor.

The skin friction, C_f , is proportional to $\mu(du/dy)$. For air flows, surface cooling decreases μ and increases du/dy . For a boundary layer at zero pressure gradient, the effect of cooling on the velocity gradients near the wall are larger than those due to viscosity and therefore skin friction increases. The increase in skin friction can also be attributed to the increase in Reynolds stress associated with the increase in density.

The extent of the changes produced is a function of the type of boundary layer. The exchange of momentum and energy in a laminar boundary layer at adiabatic wall conditions is due to molecular motion. Surface cooling leads to a fuller velocity profile in the laminar boundary layer, which in turn leads to changes in the boundary-layer profile and its integral values. Momentum and energy exchange in the turbulent boundary layer takes place through turbulent eddies. Due to the fact that the energy changes produced by heat transfer are only a small proportion of the energy exchange produced by the turbulent motion, the effect on the velocity profile and velocity gradient near to the wall is relatively small.

In general, some of the effects due to surface cooling on a flat plate boundary layer are analogous to that of boundary-layer suction, in that

boundary-layer suction also produces a transfer of energy in the boundary layer towards the surface leading to a fuller velocity profile, increased velocity gradients and skin friction, and decreased the shape factor. However, cooling also leads to a decrease in the viscosity and increases the density nears the surface resulting in relatively large increases in the 'effective' Reynolds number.

In the case of transonic flows, the boundary layer thickness and sonic height in the supersonic region are of the same order. Surface cooling, through increases in velocities near the surface, decreases sonic height and therefore the communication signals in the boundary layer. This results in a reduced shock interaction region and an increase in pressure gradients across the shock. Furthermore, the reduced boundary layer thickness moves the shock forward on the surface. However, care should be taken in experimental measurements of heat transfer effects, as surface heat transfer has been observed to introduce spurious scale effects in wind-tunnel testing⁽⁶¹⁾.

Figures 12 and 13 respectively illustrate the predicted effects of cooling on transonic periodic flow on a 14% bi-convex aerofoil^(21, 29) and on the LV2F aerofoil⁽³⁹⁾. For 14% bi-convex aerofoil (Fig. 12), computational investigations were performed with a RANS approach using a Baldwin Lomax turbulence model, at $M = 0.83$, $Re = 9 \times 10^6$, $\alpha = 0^\circ$, with temperature ratios of $T_w/T = 1$ (adiabatic) and 0.6 (cooling). A temperature ratio of 0.6 is not a practical value if cooling was to be used as a technique to control drag or buffet and therefore the results are viewed as only providing a qualitative understanding. The results shown here are for the variation of lift (Fig. 14(a)) and shock position (Fig. 14(b)) during the periodic motion. The effect of cooling in reducing the periodic motion, and therefore buffet, is clearly observed. With cooling, the movement of the shock has been virtually eliminated and is typical of the Tidjeman type A periodic motion, whereas type B periodic motion is observed in the corresponding adiabatic conditions. The results are qualitatively in agreement with experimental data⁽²¹⁾.

The effect of cooling on the transonic periodic flow over the LV2F aerofoil shows a similar effect (Fig. 13), indicating the sensitivity of periodic motion to wall temperature. It has also been demonstrated that wall heating has the direct opposite effect to cooling by promoting increased buffet levels^(21, 29).

The experimental results on a LV2F aerofoil presented in this paper are from the tests performed in the PETW at the European Transonic facility (Fig. 9(a)), where the model temperature may not have been at adiabatic wall temperature (potentially slightly higher than the adiabatic wall temperature). This has a number of implications in general for wing tunnel testing where the model temperature is not the same as the adiabatic wall temperature. However, it should be emphasised that in the ETW facility, cryogenic wind-tunnel models are generally cooled to the same temperature as the adiabatic wall temperature so as to avoid any effects associated with heat transfer (as is the case in the test cases presented here).

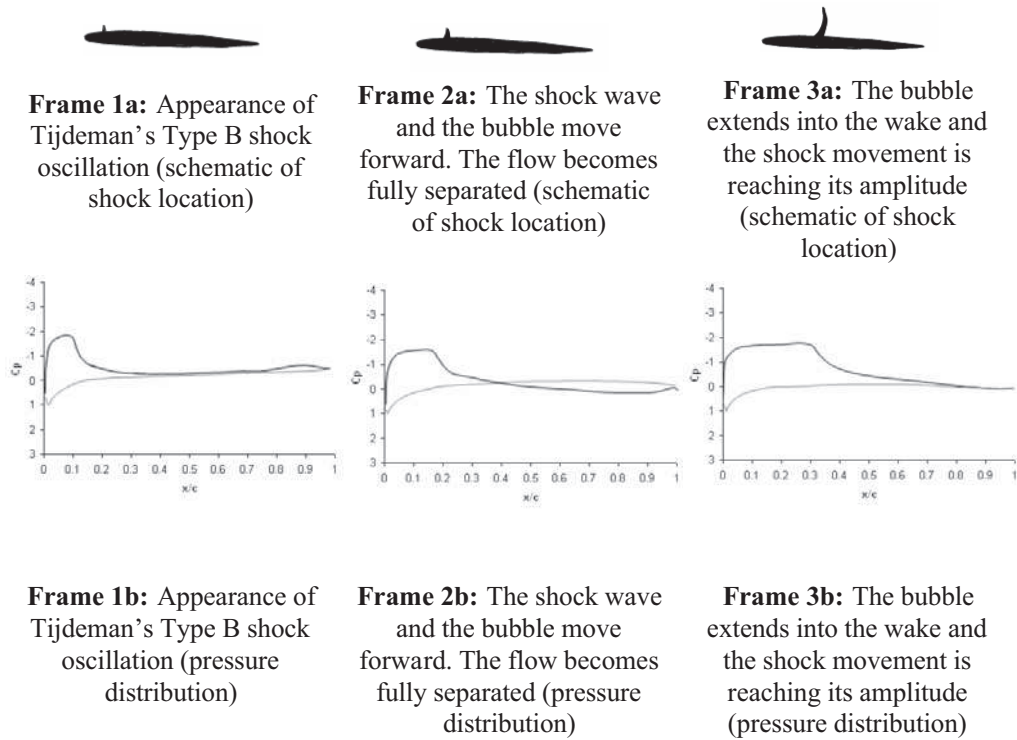


Figure 15(a). Case without bump ($k = 0.16$)^(38, 39).

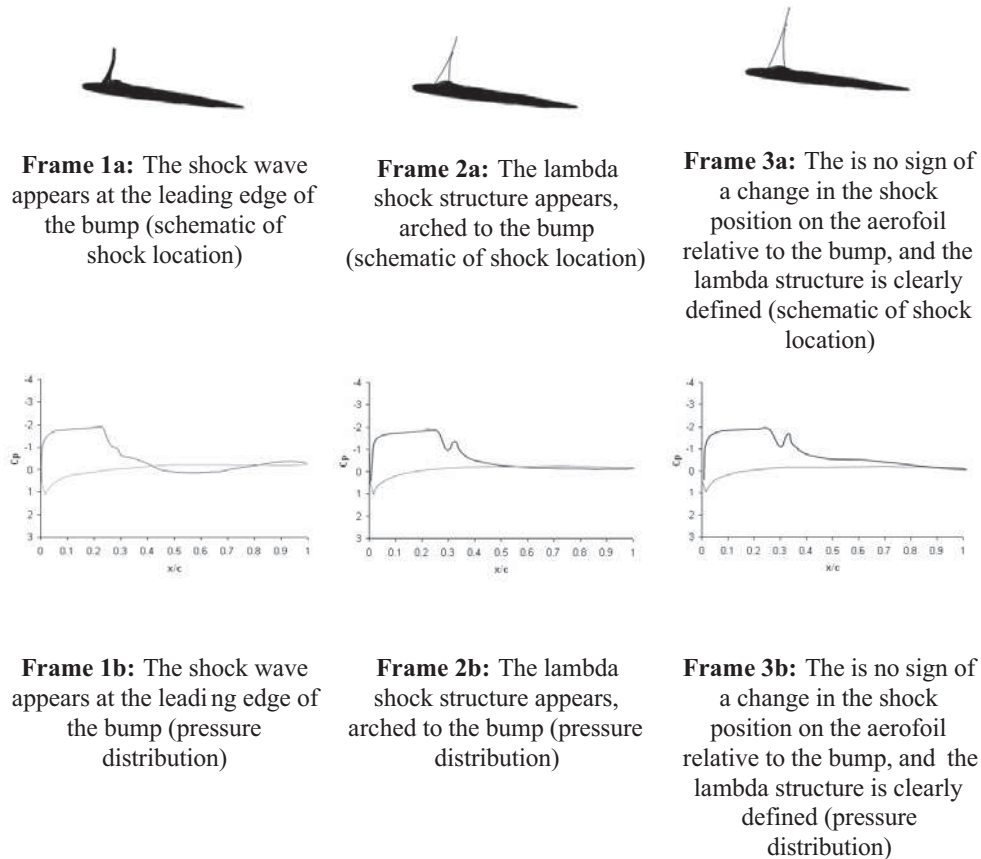


Figure 15(b). Case with bump ($k = 0.24$)^(38, 39).

Figure 15. Periodic flow over a NACA0012 aerofoil at $M_\infty = 0.7$, $Re = 9 \times 10^6$, $\alpha = 3.2^\circ$ shock waves and pressure distributions at three discrete time intervals during a period of oscillation^(38, 39).

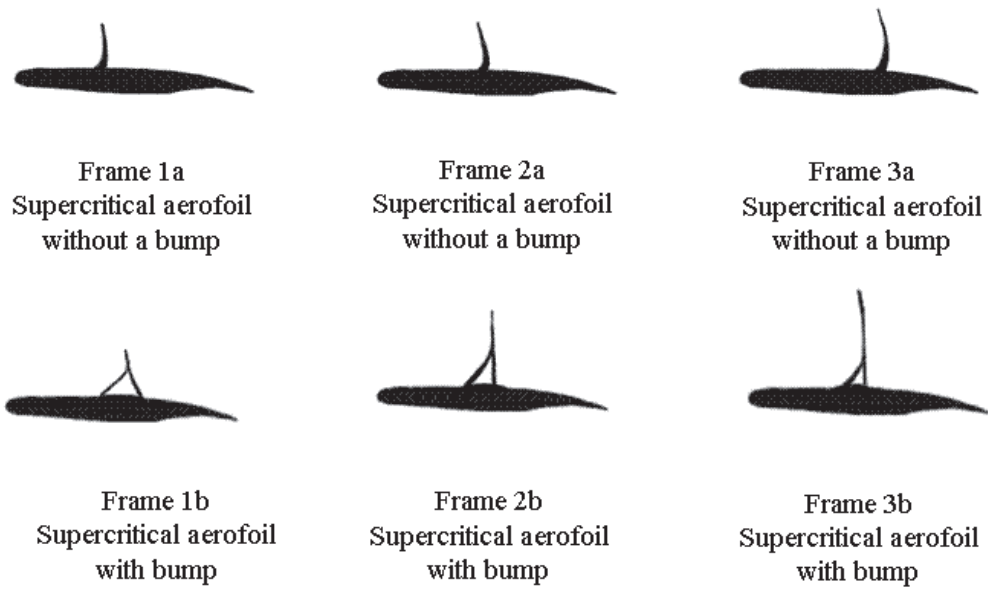


Figure 16(a). Shock waves.

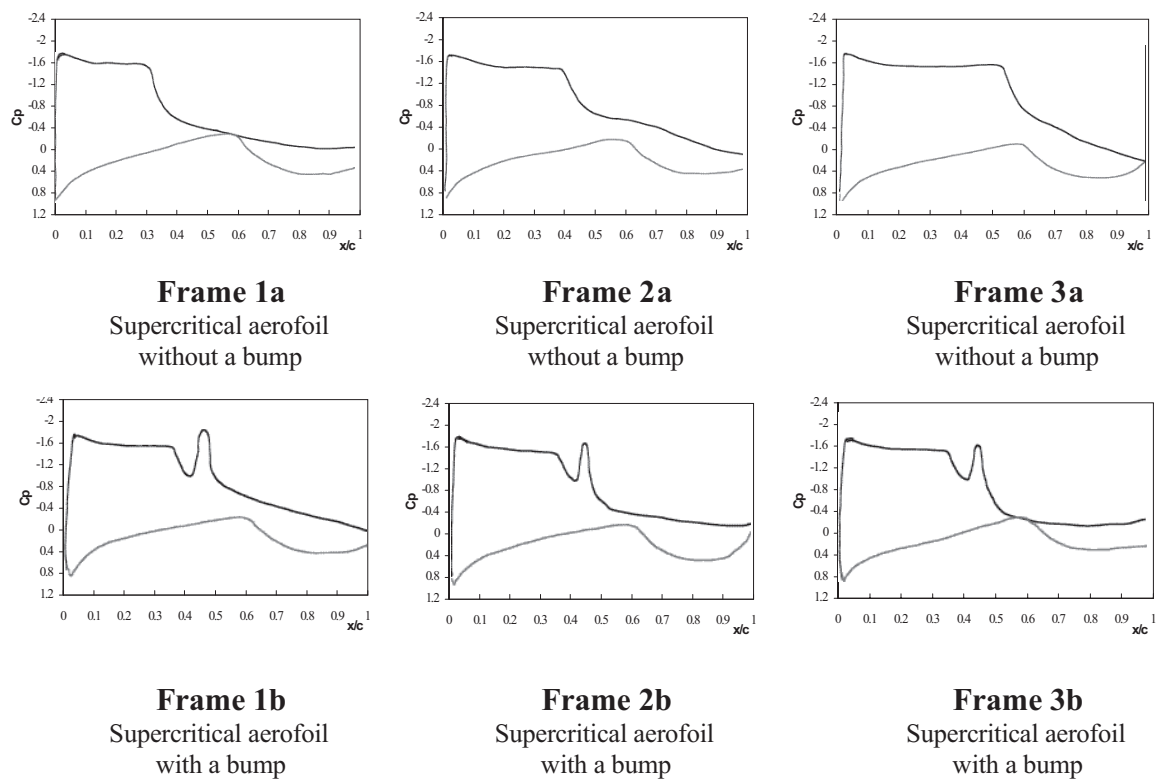


Figure 16(b). Pressure distributions.

Figure 16. Periodic motion on a supercritical aerofoil with a bump ($M = 0.74$, $Re = 10 \times 10^6$, $\alpha = 4^\circ$).

6.0 ALLEVIATION OF PERIODIC TRANSONIC FLOW BY A BUMP

In general, the buffet onset on an aerofoil is preceded by drag divergence due to boundary layer separation or formation of shock waves. Therefore methodologies that are used in the control of separation (shock induced or otherwise) could, in theory, also be used to alleviate buffet. There are several control devices proposed to reduce drag on aerofoil and wings at transonic speed (see, for example, Refs 20, 43, 65, 73), and more detail of the flow over an aerofoil with a bump can be found in⁽⁷⁴⁾. These devices are either passive or active, and include sub-layer mechanical devices, bumps, surface cooling devices, vortex generators, boundary-layer suction/blowing, continuous or pulse skewed air jets and synthetic jets. Some of the methods of flow control, including adaptive wing technology, have been discussed in detail by several researchers. One of the devices investigated for transonic shock boundary-layer interaction is the porous surface with cavity⁽⁶²⁾. The benefit of this device, however, was limited by the fact that the rapid thickening of the boundary-layer upstream of the shock, due to blowing, results in increased viscous losses in spite of any positive effect of suction downstream of the shock interaction. In principle, the concept of passive control, which produces a re-circulating flow in the region of control, is equivalent to having a contoured bump on the surface⁽⁶⁸⁾. Here the focus is on one particular type of flow control – the bump.

The contoured bump as a device for drag reduction appears to be promising^(73,74). Investigations on aerofoils with a contoured bump with a bump height to aerofoil chord ratio of 0.002-0.003, bump length to airfoil chord ratio of 0.1 to 0.3 and the bump located at the mean shock position on the aerofoil have shown that a drag reduction of 10% can be achieved. DASA-Airbus, in introducing a bump into an A340-type hybrid laminar flow wing and assuming a typical mission for such an aircraft of 600 flights per year, has determined that fuel savings of up to 2% at a cruise Mach number of 0.84 can be achieved⁽⁷⁰⁾. The reduction of drag is essentially due to the reduction in wave drag but with no corresponding increase in the viscous drag.

Generally, the control techniques used to reduce wave drag should also reduce buffet, and the use of such a bump as a control technique for buffet associated with periodic transonic flows is reviewed in this section (Figs 14-16). The test cases chosen are (a) NACA0012 aerofoil, at $M = 0.7$ and $Re = 9 \times 10^6$, $\alpha = 3.2$ degrees, transition fix at 5% and (b) LV2F aerofoil, at $M = 0.74$, $Re = 10 \times 10^6$, $\alpha = 4$ deg, transition fix at 7%. In both cases, the bump had a length of 10% and height of 0.2% of aerofoil chord and was located at the mean shock position.

Comparison of the computational results on a NACA0012 aerofoil and the same aerofoil with a bump, (Fig. 14) demonstrate that the addition of a contoured bump significantly reduces the fluctuating lift, and correspondingly, the extent of shock motion on the surface. Compared to the datum, placing a bump on the aerofoil resulted in a reduction in buffet (Fig. 14(a)) and the chordwise shock motion by 75% (Fig. 14(b)). The results also show that with the bump the frequency of shock motion is increased. The reduced frequency has increased by 50%, from 0.16 to 0.24, the mean shock position has moved from 25% chord to 35% chord – closer to the location of the bump – and the type of shock motion has changed from the Tijdeman's type B (datum aerofoil) to type A (aerofoil with a bump).

The changes in the structure of the shock interactions can be inferred by comparison of Mach number contours, pressure distributions and skin friction coefficients at typical instants in a cycle with and without the bump (Fig. 15). The results for transonic flow without a bump (Fig. 15(a)) for Mach number contours, pressure distributions, and skin friction for the NACA0012 are similar to earlier studies on that aerofoil and discussed previously in Section 1. The shock interaction is spread over a narrow region on the aerofoil surface. At this low Reynolds number relative to free flight conditions, when the shock is well upstream during a cycle, both the

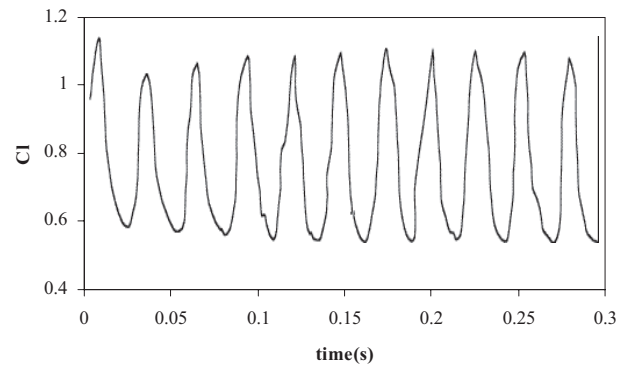


Figure 17(a). No control technique⁽⁴⁰⁾.

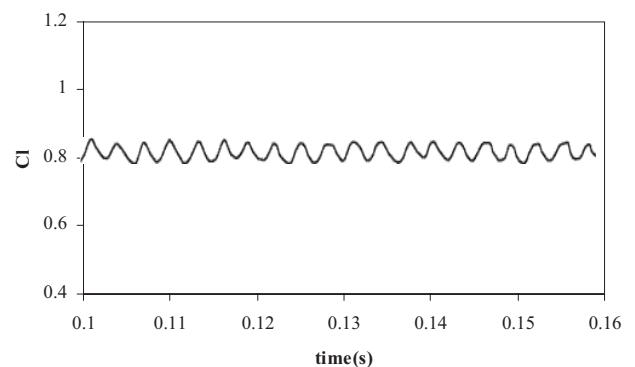


Figure 17(b). Buffet alleviation by Contour Bump technique⁽⁴⁰⁾.

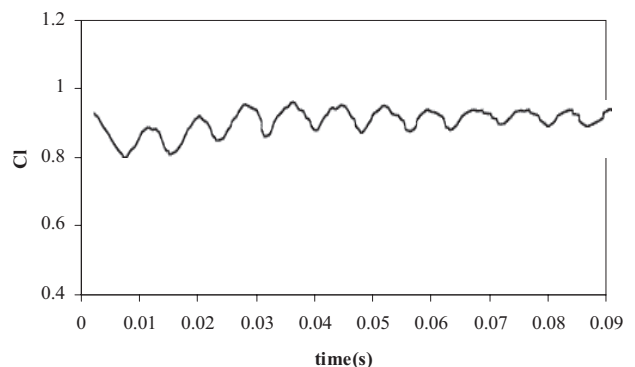


Figure 17(c). Buffet alleviation by Cavity technique⁽⁴⁰⁾.

Figure 17. Alleviation of buffet on supercritical aerofoil ($M = 0.74$, $Re = 10 \times 10^6$, $\alpha = 4^\circ$) Tr 18% (a) datum, (b) bump, (c) cavity (based on Ref. 40).

pressure distributions and Mach number contours show the existence of trailing edge separation. However, the Mach number contours on the NACA0012 with a contoured bump (Fig. 15(b)) show that at all time instants a lambda type of shock structure with two distinct legs exists, with the leading edge of the lambda close to the leading edge of the bump. The pressure distributions confirm this shock structure, and also show that the variation of the trailing-edge pressure during the periodic motion is relatively small. The observed structure is similar to that on an aerofoil with passive boundary-layer control using a plenum and a cavity⁽⁶⁹⁾. It appears, therefore, that generation of an oblique shock by a device placed in supersonic region of aerofoil stabilises the shock position and therefore reduces buffet. The periodic motion observed is primarily due to the motion of the second, weaker leg of the lambda shock on the bump.

The increase in frequency on an aerofoil with a bump can be attributed to the location of the mean shock further aft, thus reducing the distance between the mean shock position and the trailing edge, which leads to a reduction in the time required for communication of signals.

However, it was observed^(38,39) that the benefit of the bump in reducing buffet on the NACA0012 was relatively small for incidence higher than 6 degrees and where the shock is well upstream on the aerofoil. The values of lift, drag and moment coefficients are reduced only marginally under these conditions. This can be attributed to the fact that at a larger incidence, there is significant boundary-layer separation and the bump is partially or fully submerged in the separated flow making it ineffective.

The effects of a bump on a supercritical aerofoil (Figs 16 and 17) are similar, qualitatively, to those observed on NACA0012 aerofoil. On a supercritical aerofoil without the bump, there is a large chord-wise motion of the shock wave during a cycle (Figs 16(a) and 16(b)) with corresponding large amplitude buffet (Fig. 17(a)). With the bump (Figs 16(a) and 16(b)), as in the case of NACA0012 aerofoil, the shock has a clear lambda structure with the leading edge of the lambda located at the leading edge of the bump. However, in this case the second leg of the lambda, although stable, is stronger relative to the case without the bump, indicating that the optimum position of the bump for alleviation of buffet may not be same for reducing drag. Further, it should be noted that the aerofoil at this low Reynolds numbers with the shock well upstream is subjected to trailing edge separation. The geometry and location of the bump for a trade off between drag reduction and buffet alleviation requires further investigation, particularly at much higher Reynolds numbers than those presented here.

A comparison of lift coefficients (Fig. 17) for transonic flow over an aerofoil with a bump with that over an aerofoil with a porous surface and a cavity indicates that either one of the two devices located at the mean shock position can be used to alleviate the buffet. However, there are differences in the achieved drag reduction. While both devices reduce wave drag, the bump does not increase viscous drag whereas a porous surface tends to lead to an increase in skin friction drag. The net gain with the former is larger than the latter. However, both devices are effective only when the shock is well located in the device. One way to increase the effectiveness of the bump when the shock position changes would be to use a deformable bump, but this could lead to additional complexity in design and detailed structural analysis⁽⁷⁵⁾, as well as a potential increase in wing production cost

6.0 CONCLUDING REMARKS

The paper has reviewed the current understanding of periodic transonic flow over circular, NACA0012 and supercritical aerofoils and the use of devices, such as the bump, to control the periodic motion.

The current understanding of the periodic transonic flows over aerofoils is that with the sudden thickening of the boundary layer, the foot of the shock leads to an effective change in geometry which in turn triggers the periodic shock motion. The frequency of the periodic motion can be predicted with reasonable accuracy. However, there are uncertainties in predicting buffet boundaries associated with this type of flow regime. The periodic motion is sensitive to the boundary-layer transition location, and is significantly reduced when the transition occur either in the region of or just upstream of shock motion. A control device which is aimed at weakening the shock wave or thickening the boundary layer, which generates of an oblique shock, can alleviate buffet. The buffet amplitude due to periodic flow can be virtually eliminated by a contoured bump or a cavity (10% aerofoil chord length and 0.2% height) located in the region of periodic flow. Such control devices also have the benefit of moving the buffet frequency away from the

structural frequencies which could be potentially damaging. Wall cooling transfers energy from the mainstream to the near wall region of the boundary, which makes the boundary layer less sensitive to separation and therefore reduces buffet, while heating has the opposite effect to cooling by promoting increased buffet.

A bump can also be used for drag reduction in transonic flows. There has been extensive investigation of the use of a bump on drag reduction on aerofoil and wings in transonic flows. The limitations in these investigations have been due in part to the current RANS approach to turbulence modelling. With the current state-of-the-art, while the existing turbulence models are adequate for viscous flows with boundary layers attached or mildly separated, prediction of three dimensional flows with large separation is beyond current techniques. CFD methods currently available, however, are adequate for understanding effects and optimising the control devices such as bump or cavity for drag reduction and buffet alleviation. Airbus studies have shown that with a bump, a large reduction of 2% in fuel burn can be obtained in a flight condition where the wave drag is significant. However, with the single-point design, and where the shock Mach number on the wing is relatively low, the wave drag is not significant enough to warrant further investigation into the placement of a bump on the wing surface. Currently there is revitalised interest in laminar flow aircraft for drag reduction and fuel consumption due to heightened environmental awareness. As the laminar boundary-layer can separate even under mild adverse pressure gradients, laminar boundary-layer shock interactions have to be avoided in design. Aerodynamic design with a laminar boundary-layer up to the positioning of the bump, followed by transition, either free or fixed, upstream of the shock is a possibility. The placement of a bump to reduce drag or buffet, with the current technology, could add to weight and overall complexity, but the evolution of new technology could alleviate this problem, and as such the net gain of employing such a technique on the overall aircraft performance is worth detailed investigations.

ACKNOWLEDGEMENTS

The authors would like to thank EPSRC, Bombardier and the Royal Academy of Engineering who provided the financial support for these investigations.

REFERENCES

1. ARGUELLES, P., BISCHOFF, M., BUSQUIN, P., DROSTE, B.A.C., EVANS, R., KROLL, W., LAGARDERE, J.L., LINA, A., LUMSDEN, J., RANQUE, D., RASMUSSEEN, S., REUTLINDER, P., ROBINS, R., TERHO, H. and WITTLÖV, A. European Aeronautics: A Vision for 2020, Report of the Group of Personalities, The European Commission, January 2001
2. McDEWITT, J.B., LEVY, JR L.L. and DIEWART, G.S. Transonic periodic flow about a thick bi-convex aerofoil, *AIAA J*, **14**, 1976, pp 606-613
3. MAGNUS, R. and YOSHIKARA, H. Transonic oscillating flap, AIAA 9th Fluid and Plasma Dynamics Conference, San Diego, USA, paper 76-327, July 1976.
4. TIDEEMAN, H. Investigation of the transonic flow around oscillating airfoils, National Aerospace Lab, The Netherlands, NLR TR-77-090U, 1977.
5. SEEGMILLER, H.L., MARVIN, J.G. and LEVY, JR, L.L. Steady and unsteady transonic flow, AIAA paper 78-160, 1978.
6. LEVY, JR, L.L. Experimental and computational steady unsteady transonic flows about a thick airfoil, *AIAA J*, 1978, **16**, pp 564-572.
7. WANG, H., HWANG, H.C. and PI, W.S. Transonic buffet behaviour of Northrop F-5A Aircraft AGARD R624, 1974.
8. McDEVITT, J.B. Supercritical flow about a thick circular-arc airfoil. NASA-TM-78549, National Aeronautics and Space Administration, January 1979.
9. MABEY, D.G. Oscillatory flow from shock induced separation on biconvex airfoils of varying thickness in ventilated wind-tunnels. AGARD CP 296, boundary-layer effects on unsteady air-loads, Aix-en-Provence, France, paper 11, 14-19 September 1980, pp 1-14.

10. LE BALLEUR, C. Computation of flows including viscous interactions with coupling methods. General Introduction Lecture 1, AGARD CP-291, computation of viscous-inviscid interactions, United States Air Force Academy. Colorado Springs Colorado, USA, 29 September-1 October 1980.
11. SELEROWICZ, W.C. and SZUMOWSKI, A.P. Airflow unstabilities induced by background flow oscillations. *Experiments in fluids*, 2002, **32**, pp 441-446.
12. MABEY, D.G., WELSH, B.L. and CRIPPS, B.E. Periodic flows on a rigid 14% thick biconvex wing at transonic speeds. TR 81059, Royal Aircraft Establishment, May 1981.
13. McDEVITT, J.B. and OKUNO, A.F. Static and dynamic pressure measurements on a NACA 0012 Airfoil in the Ames High Reynolds Number Facility, NASA TP-2485, June 1985.
14. RAGHUNATHAN, S. Passive control of shock boundary-layer interaction, *Progress in Aerospace Sciences*, 1988, **25**, pp 271-296.
15. GIRODROUX-LAVIGNE, P. and LE BALLEUR, J.C. Time-consistent computation of transonic buffet over airfoils. Proceedings of 16th Congress of the International Council of the Aeronautical Sciences, ICAS 88-5.52, 1988, pp 779-787.
16. GIBB, J. The cause and cure of periodic Flows at transonic speeds, ICAS, Paper 3, 1988, **10**, (1).
17. LEE, B.H.K. Oscillatory shock motion caused by transonic shock boundary-layer interaction. *AIAA J*, 1990, (28), pp 942-944.
18. RAGHUNATHAN, S., HALL, D.E. and MABEY, D.G. Alleviation of Shock oscillations in transonic flow by passive control. *Aeronaut J*, 1990, **94**, (937), pp 245-250.
19. MABEY, D.G. Effects of heat transfer in aerodynamics and possible implications for wind-tunnel tests, *Progress in Aerospace Sciences*, **27**, (4), pp 267-303, 1991.
20. BENNET, M.R., DANSBERRY, B.E., FARMER, M.G., ECKSTROM, C.V., SEIDEL, D.A. and RIVERA, J.A. Transonic shock-induced dynamics of flexible wing with a thick circular-arc aerofoil, AIAA paper 91-1107, 1991.
21. RAGHUNATHAN, S., ZARIFI-RAD, F. and MABEY, D.G. Effect of model cooling in transonic periodic flow. *AIAA J*, 1992, **30**, (8), pp 2080-2089.
22. EDWARDS, J. Transonic shock oscillations calculated with a new interactive boundary-layer coupling method, AIAA Paper 93-0777, 1993.
23. RAGHUNATHAN, S. and MITCHELL, D. Computed effects of heat transfer on transonic flows. *AIAA J*, 1995, **33**, (11), pp 2120-2127.
24. RUMSEY, C.L., SANETRIK, M.D., BIEDRON, R.T., MELSON, N.D. and PARLETTE, E.B. Efficiency and accuracy of time-accurate turbulent Navier-Stokes computations. AIAA paper 95-1835, 1995.
25. BARTEL, R.E. and ROTHMAYER, A.P. An IBL approach to multi-scaled shock induced oscillations, AIAA 26th Fluid Dynamics Conference, San Diego, USA, paper 95-2157, 1995.
26. STANEWSKY, E. EUROSCHOCK I AND II: A SURVEY. Drag reduction by shock and boundary-layer control, IUTAM Symposium on Mechanics of passive and active flow control, Göttingen, 1998, pp 35-43.
27. RAGHUNATHAN, S., MITCHELL, R.D. and GILLAN, M.A. Transonic shock oscillations on NACA0012 aerofoil, *Shock Waves*, 1998, **8**, pp 191-202.
28. LEE, B.H.K., Oscillatory shock motion caused by transonic shock boundary-layer interaction. *AIAA J*, 1989, **28**, (5), pp 942-944.
29. RAGHUNATHAN, S., GILLAN, M.A., COOPER, R.K., MITCHELL, R.D. and COLE, J.S. Shock Oscillations on biconvex aerofoils, *Aerospace Science and Technology*, 1999, **3**, (1), pp 1-9.
30. MITCHELL, D.A., COOPER, R.K. and RAGHUNATHAN, S. Effect of heat transfer on periodic transonic flows, *Aeronaut J*, July 1999, **103**, (1025), pp 329-337.
31. LEE, B.H.K. Self-sustained shock oscillations on airfoils at transonic speed, *Progress in Aerospace Sciences*, 2001, **37**, pp 147-196.
32. LEE, B.H.K. Transonic buffet on a supercritical aerofoil, *Aeronaut J*, 1990, **94**, (935), pp 143-152.
33. LEE, B.H.K., ELLIS, F.A. and BUREAU, J. Investigation of the buffet characteristics of two supercritical airfoils, *J Aircr*, 1989, **26**, (8), pp 731-736.
34. LEE, B.H.K., MURTY, H., and JIANG, H. Role of kutta waves on oscillatory shock motion on an airfoil, *AIAA J*, 1994, **32**, (4), pp 789-795.
35. BARTELS, R.E. Flow and turbulence modeling and computation of shock buffet onset for conventional and supercritical airfoils, NASA TP-1998-206908, February 1998.
36. BARTELS, R.E. and EDWARDS J.W. Cryogenic tunnel pressure measurements on a supercritical airfoil for several shock buffet conditions, NASA TM-110272, 1997.
37. BARTEL, R.R. Computation of shock buffet onset on conventional and supercritical aerofoil., AIAA Aerospace Sciences meeting, AIAA paper 97-0833, Reno, Nevada, USA, January 1997.
38. TULITA, C., RAGHUNATHAN, S. and BENARD, E. Control of transonic periodic flow on NACA0012 aerofoil by contour bumps. IUTAM Symposium Transsonicum IV, pp 291-297, Göttingen, 2002.
39. TULITA, C., BENARD E. and RAGHUNATHAN S. Transonic periodic flow subject to adaptive bump. AIAA 41st Aerospace Sciences Meeting and Exhibit, Reno, Nevada, USA, paper 2003-0444, 2003.
40. TULITA, C., TURKBAYER, E. and RAGHUNATHAN, S. Investigation of the influence of turbulent transition on periodic transonic flow. Symposium Integrated CFD and Experimental Aerodynamics, Cranfield, UK, 5-6 September 2005.
41. BARAKOS, G. and DRIKAKIS, D. Numerical simulation of transonic buffet flows using various turbulence closures, *Int J Heat and Fluid Flow*, **21**, (5), 2000, pp 620-626.
42. XIAO, Q., TSAI, H.M., LIU, F. Numerical study of transonic buffet on a supercritical airfoil, *AIAA J*, **44**, (3), March 2006, pp 620-628.
43. RAGHUNATHAN, S., GILLAN, M.A. and MITCHELL, R.D. Studies on alleviation of buffet in periodic transonic flow, *AIAA J*, **35**, (12), 1997, pp 1890-1891.
44. PULLIAM, T. Time accuracy and the use of implicit methods, AIAA paper 93-3360-CP, July 1993.
45. JAMESON, A. Time dependent calculations using multigrid, with applications to unsteady flows past airfoils and wings, AIAA paper 91-1596.
46. BALDWIN, B. and LOMAX, H. Thin layer approximation and algebraic model for separated turbulent flow, AIAA paper 78-257.
47. SPALART, P.S. and ALLMARAS, S. A one equation turbulence model for aerodynamic flows, AIAA paper 92-0439, 1992.
48. VAN LEER, B. Flux vector splitting for the Euler equations, ICASE Report 82-30, 1982.
49. MULDER, W.A. and VAN LEER, B. Implicit upwind methods for the Euler equations, AIAA paper 83-1930, 1983.
50. KOCH, S. and ROSEMAN, H. Experimental investigations of shock oscillations in cryogenic Ludweig tube, DLR report, 1B, 224-2002CO3, 2002.
51. DEIWERT, G.S. Numerical simulation of high Reynolds number transonic flows, *AIAA J*, 1975, **13**, pp 1354-1359.
52. STEGER, J.L. Implicit finite-difference simulation of flow about arbitrary two-dimensional geometries. *AIAA J*, 1978, **16**, pp 679-686.
53. BATINA, J.T. Unsteady transonic small-disturbance theory including entropy and vorticity effects, *J Aircr*, June 1989, **26**, pp 531-538.
54. GREEN, J.E., WEEKS, D.J. and BROOMAN, J.W.F. Prediction of turbulent boundary layers and wakes in compressible flow by a lag-entrainment method. R&M No. 3791, British Aeronautical research Council, 1977.
55. MELNIK, R.E. and BROOK, J.W. The Computation of Viscid/Inviscid Interaction on Airfoils With Separated Flow. Third Symposium on Numerical and Physical aspects of Aerodynamic Flows, California State University, 1985, pp 1-21-1-37.
56. CARTER, J.E. A new boundary-layer inviscid interaction technique for separated flows. AIAA paper 79-1450.
57. PAPPAS, C.C. Measurement of heat transfer in the turbulent boundary layer on a flat plate in supersonic flow and comparison with skin friction results, NACA TN 3222.
58. SPALDING, D.B. and CHI, S.W. The drag of a compressible turbulent boundary layer on a smooth flat plate with and without heat transfer, *J Fluid Mechanics*, **18**, pp 117-143.
59. BACK, L.H. and CUFFEL, R.F. Shock wave/turbulent boundary-layer interactions with and without surface cooling, *AIAA J*, **14**, (4), pp 526-532.
60. VAN DRIEST, E.R. *Convective heat transfer in gases. Turbulent flows and heat Transfer in High Speed Aerodynamics and Jet Propulsion*, Section F, **5**, Oxford University Press, 1969, UK.
61. GREEN, J.E., WEEKS, D.J. and PUGH, P.G. Heat transfer as a source of spurious scale effects in subsonic and transonic wind-tunnels, ARC 38182, May 1979.
62. DOUGHERTY, N.S. and FISHER, D.F. boundary-layer transition on a 10 cone: wind-tunnel and flight test correlation. AIAA Paper 80-01544, 1980.
63. LIEPMANN, H.W. and FILA, G.H. Investigations of effect of surface temperature and single roughness elements on boundary-layer transition. NACA TN 1196, 1947.
64. FRISHETT, J.C. Incipient Separation of a Supersonic Turbulent Boundary Layer Including Effects of Heat Transfer, PhD Thesis, University of California, USA, 1971.
65. INGER, G.R., LYNCH, F.T and FAUCHER, M.F. A theoretical and experimental study on non-adiabatic wall effects on transonic shock-boundary-layer interaction. AIAA Paper 83-1421, 1983.

66. DELERY, J.M. Shock wave-turbulent boundary-layer interaction and its control. *Progress in Aerospace Sciences*, 1985, **22**, pp 209-280.
67. RAGHUNATHAN, S. Passive control of shock boundary-layer Interaction, *Progress in Aerospace Sciences*, 1988, **25**, pp 271-296.
68. ASHILL, P.R., FULKER, J. and SHIRES, A. A novel technique for controlling shock strength of laminar-flow aerofoil sections, Proceed of the First European Forum on Laminar Flow Technology, DGLR-Bericht 92-06, 1992.
69. STANEWSKY, E., FULKER, J., DELERY, J. and GEIBLER, J. Drag Reduction by passive Shock Control-Results of the project EUROSHOCK, AER2-CT92-0049, *Notes on Num Fluid Mech*, **56**, Vieweg Verlag, 1997.
70. STANEWSKY, E. EUROSHOCK I AND II: A SURVEY. Drag Reduction by Shock and boundary-layer Control, IUTAM Symposium on Mechanics of Passive and Active Flow Control, Gottingen, 35-43, 1998.
71. DELERY, J. and BUR, R. The physics of shock wave/boundary-layer interaction control: last lessons learned. ECCOMAS TP2000-181, Barcelona, Spain, 11-14 September 2000.
72. SOMMERER, A., LUTZ, T. and WAGNER, S. Design of adaptive transonic airfoils by means of numerical optimization, ECCOMAS 2000, Barcelona, Spain, September 2000.
73. STANEWSKY, E., DELERY, J., FULKER, J. and MATTEIS, P. DE Drag reduction by shock and boundary-layer control. Results of the project EUROSHOCK II BRPR-95-76, Notes on numerical fluid mechanics and multidisciplinary design, **80**, Springer, 2002.
74. ASHILL, P.R., FULKER, J.L. and HACKETT, K.C. A review of recent developments in flow control, *Aeronaut J*, May 2005, **105**, (1095), pp 205-232.
75. WADEHN, A., SOMMERER, TH LUTZ, FOKIN, D., PRISCHOW and WAGNER, S. Structural concepts and aerodynamic design of shock control bumps, ICAS Proceedings, Canada, September 2002.